



Phase composition and phase transformation in Bi(Sb,Nb,Ta)O₄ system

Di Zhou*, Li-Xia Pang, Hong Wang, Xi Yao

Electronic Materials Research Laboratory, Key Laboratory of the Ministry of Education, Xi'an Jiaotong University, No. 28 Xianning West Road, Xi'an 710049, Shaanxi, China

ARTICLE INFO

Article history:

Received 17 June 2009

Received in revised form

23 July 2009

Accepted 27 July 2009

Available online 6 August 2009

Keywords:

Electronic material

X-ray diffraction (XRD)

Dielectrics

Sintering

Bi(Sb,Nb,Ta)O₄

ABSTRACT

In this work Bi(Sb_xNb_yTa_z)O₄ ($x + y + z = 1$) samples are prepared using mixed-oxide method. A pseudo-ternary phase diagram of Bi(Sb,Nb,Ta)O₄ system is given below the melting point. It is composed of a monoclinic phase region, an orthorhombic phase region and a monoclinic–orthorhombic co-existing phase region. In the orthorhombic phase region, the transformation from orthorhombic to triclinic phase is found to be sensitive to the composition and sintering temperature. Both the transformation from monoclinic to orthorhombic structure and the transformation from orthorhombic to triclinic structure have been studied by the cell parameters.

Crown Copyright © 2009 Published by Elsevier Masson SAS. All rights reserved.

1. Introduction

As early as 1960s, the XRD analysis of the A³⁺B⁵⁺O₄ compositions (A = Bi³⁺ or Sb³⁺, and B = Nb⁵⁺, Ta⁵⁺, Sb⁵⁺ or Bi⁵⁺) showed that all the compounds are isostructural, though various modifications are possible [1–7]. Because of the valence instability of Sb³⁺ and Bi⁵⁺, which means that Sb³⁺ and Bi⁵⁺ are not stable during sintering course in air atmosphere (Sb³⁺ is easy to be oxygenized to Sb⁵⁺ and Bi⁵⁺ is easily reducible), only the Bi(Sb,Nb,Ta)O₄ powders, ceramics or single crystals have been studied widely covering a broad scope of dielectric (ferroelectricity, ferroelasticity, anti-ferroelectricity [8–11], low temperature co-fired ceramics for microwave use [12–16]) and optical study (photocatalyst [17–19]). Since the microwave dielectric properties of BiNbO₄ ceramic were first reported by Kagata et al. in 1992 [12], many researchers performed a series of studies on BiNbO₄ ceramic to modify its properties and lower its sintering temperature for the application in low temperature co-fired ceramic (LTCC) technology [20–23]. Subsequently Huang et al. reported the microwave dielectric properties of BiTaO₄ ceramic with CuO addition [13]. Wang et al. used Ta⁵⁺ and Sb⁵⁺ to substitute for the Nb⁵⁺ in BiNbO₄ and obtained adjustable permittivity and temperature coefficients [14,24]. In our recent studies, we reported the good microwave dielectric properties of BiSbO₄ and Bi(Sb,Ta)O₄ ceramics [15,16]. In 2001, Zou et al. [19]

studied the photocatalytic and photophysical properties of BiTa_{1-x}Nb_xO₄ ($0 \leq x \leq 1$) solid solutions and found their promising application in photocatalyst. BiSbO₄ was also reported in detail as a novel p-block metal oxide, which possesses a visible light response for the photocatalytic degradation of methylene blue by Lin et al. [17].

Based on the studies on A³⁺B⁵⁺O₄ (A = Bi³⁺, and B = Nb⁵⁺, Ta⁵⁺, Sb⁵⁺) family's properties and structures, it attracts us to study the phase relationship between BiNbO₄, BiTaO₄ and BiSbO₄ compounds. Roth and Waring [2,3] first reported the existence of the low temperature orthorhombic modification (α phase) of BiNbO₄ and powder X-ray diffraction data showed the low temperature form is similar to that of stibotantalite type (SbTaO₄) structure. They also reported that the low temperature α -BiNbO₄ transformed irreversibly to the triclinic form (β phase) at around 1020 °C (although this conclusion "irreversibility" was proved to be dubious in our previous work [7], it does not affect the discussions in this work and the related experiment on the "irreversibility" will be discussed in another work). Keve and Skapski [4,5] grew a single crystal of β -BiNbO₄ in 1973 and found its structure along the c -axis consisted of layers of [Bi₂O₂] units separated by puckered sheets of [NbO₆] octahedra. The BiTaO₄ was also found to transform from a low temperature orthorhombic α phase to a high temperature triclinic β phase at around 1140 °C [1,3]. Kennedy [25] reported a Rietveld refinement of X-ray powder diffraction study of BiSbO₄ and found that it belongs to a monoclinic structure with the space group $I2/c$. Zou et al. [18,19] studied the solid solution of BiTa_{1-x}Nb_xO₄ ($0 \leq x \leq 1$) and found a discontinuous phase transformation from a orthorhombic phase to a triclinic phase in ceramic

* Corresponding author. Tel.: +86 29 82668679; fax: +86 29 82668794.

E-mail addresses: zhoudi1220@gmail.com (D. Zhou), hwang@mail.xjtu.edu.cn (H. Wang).

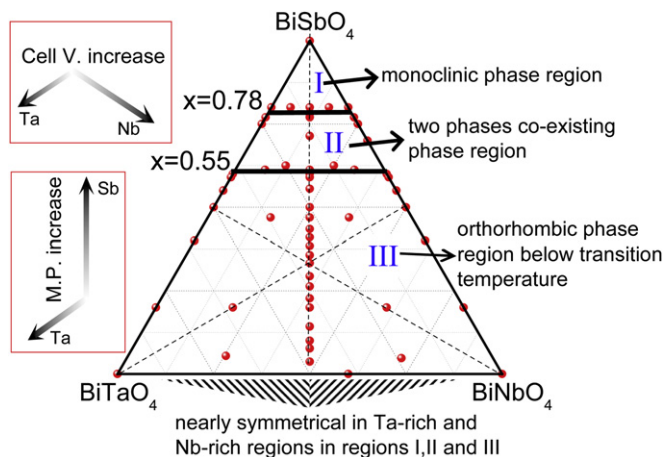


Fig. 1. Pseudo-phase diagram of $\text{Bi}(\text{Sb}_x\text{Nb}_y\text{Ta}_z)\text{O}_4$ ($x + y + z = 1$) system (I – monoclinic phase region below the melting point, III – orthorhombic phase region below transition temperature (in fact this region must be studied as a function of sintering temperature as discussed in paragraph “Results and discussions”), II – monoclinic and orthorhombic co-existing phase region below the melting point, M.P. – melting point, cell V – cell volume).

samples sintered at $1100\text{ }^\circ\text{C}$. Lee et al. [26] also studied the structure of $\text{BiTa}_{1-x}\text{Nb}_x\text{O}_4$ and they found that pure orthorhombic phase could be obtained by prolonged heating at relatively low temperatures ($\leq 970\text{ }^\circ\text{C}$) and the amounts of triclinic phase were sensitive to the temperature. An unusual variation in the cell parameters in the orthorhombic was also observed. As the Nb content increased, the cell parameters a and c increased whereas the parameter b decreased, which was attributed to the bonding difference of the Nb 4d and Ta 5d. The phase composition of $\text{Bi}(\text{Sb},\text{Ta})\text{O}_4$ and $\text{Bi}(\text{Sb},\text{Nb})\text{O}_4$ in the monoclinic region and orthorhombic region were studied in Wang’s and our previous work [16,24,27]. The monoclinic solid solution could be formed when $x \leq 0.2$ and pure orthorhombic solid solution could be obtained when $x > 0.5$ in the $\text{Bi}(\text{Sb}_{1-x}\text{Ta}_x)\text{O}_4$ and $\text{Bi}(\text{Sb}_{1-x}\text{Nb}_x)\text{O}_4$ systems. Considering the important role played by the quinquivalent ions $(\text{Sb},\text{Nb},\text{Ta})^{5+}$ in many fields [16,26,28], in the present work we prepared a number of compositions especially near the phase boundary regions in the $\text{Bi}(\text{Sb}_x\text{Nb}_y\text{Ta}_z)\text{O}_4$ ($x + y + z = 1$) system to obtain a pseudo-diagram and study the relationship between the phase composition, structure and the sintering temperature.

2. Experimental details

The pure powders of BiNbO_4 , BiTaO_4 and BiSbO_4 were first prepared via the mixed-oxide method using starting materials of Bi_2O_3 (>99%, Shu-Du Powders Co. Ltd, China), Nb_2O_5 (>99%, Zhu-Zhou Harden Alloys Co., Ltd., China), Ta_2O_5 (>99%, Guo-Yao Co. Ltd., Shanghai, China) and Sb_2O_3 (>99%, Xi’an of China, State Chemical, Xi’an, China) respectively. The BiNbO_4 , BiTaO_4 and BiSbO_4 powders were calcined at $800\text{ }^\circ\text{C}$, $850\text{ }^\circ\text{C}$ and $850\text{ }^\circ\text{C}$ for 4 h respectively. Then the different compositions were prepared by mixing the BiNbO_4 , BiTaO_4 and BiSbO_4 powders according to $\text{Bi}(\text{Sb}_x\text{Nb}_y\text{Ta}_z)\text{O}_4$ ($x + y + z = 1$). Every composition was re-milled for 4hrs, dried and pressed into pellets. The pellet samples were sintered for 2 h under air atmosphere in the temperature range from $900\text{ }^\circ\text{C}$ to the melting points (the melted samples were not studied in this work) with a heating rate about $3\text{ }^\circ\text{C}/\text{min}$ and then cooled down to the room temperature. The natural cooling rate was about $5\text{--}7\text{ }^\circ\text{C}$ per minute. The crystalline structures of the samples (ground powders) were investigated using an X-ray diffractometry with Cu $K\alpha$

radiation (Rigaku D/MAX-2400 X-ray diffractometry, Japan) and the cell parameters were calculated using JADE software.

3. Results and discussions

Based on the analysis on a number of $\text{Bi}(\text{Sb}_x\text{Nb}_y\text{Ta}_z)\text{O}_4$ ($x + y + z = 1$) samples, a pseudo-ternary phase diagram is given in Fig. 1. This diagram included three regions marked with I, II and III respectively. In Sb-rich region (region I, $x \geq 0.78$ in $\text{Bi}(\text{Sb}_x\text{Nb}_y\text{Ta}_z)\text{O}_4$), all the compositions belong to monoclinic structure in the temperature range from $900\text{ }^\circ\text{C}$ till their melting points no matter the different ratio of y to z , which was attributed to the similar ionic radii of Nb^{5+} and Ta^{5+} . In an octahedral environment (coordination number = 6), the Nb^{5+} and Ta^{5+} both have a ionic radius of 0.64 \AA , which are bigger than that of Sb^{5+} (0.60 \AA) [29]. As x value decreased from 1 to 0.78 in $\text{Bi}(\text{Sb}_x\text{Nb}_y\text{Ta}_z)\text{O}_4$, the average ionic radius of B^{5+} increased from 0.60 \AA to about 0.609 \AA . All the compositions in region III ($x \leq 0.55$) in $\text{Bi}(\text{Sb}_x\text{Nb}_y\text{Ta}_z)\text{O}_4$ system belong to a orthorhombic phase, which is also symmetrical in Ta-rich and Nb-rich areas, from $900\text{ }^\circ\text{C}$ till their phase transformation temperatures. In the region III, the phase transformation from orthorhombic phase to triclinic phase is sensitive to both the composition and the sintering temperature, which will be discussed in detail in the next paragraph. As the x value decreased from 0.55 to 0 in $\text{Bi}(\text{Sb}_x\text{Nb}_y\text{Ta}_z)\text{O}_4$, the average ionic radius of B^{5+} increased from 0.618 \AA to 0.64 \AA . Both the monoclinic and orthorhombic phases were observed when $0.55 \leq x \leq 0.78$ in the region II. The typical XRD patterns of the monoclinic phase, mixed phases and orthorhombic phase are shown in Fig. 2(a). The melting points of $\text{Bi}(\text{Sb}_x\text{Nb}_y\text{Ta}_z)\text{O}_4$ increased as the Sb amount increased. Increase of Ta amount would also induce slight increase of the melting point. Cell volumes of $\text{Bi}(\text{Sb}_x\text{Nb}_y\text{Ta}_z)\text{O}_4$ would increase obviously as the amount of (Nb,Ta) increased because of their bigger ionic radii than that of Sb^{5+} .

The lattice parameters of monoclinic $\text{Bi}(\text{Sb}_{0.78}\text{Nb}_{0.11}\text{Ta}_{0.11})\text{O}_4$ and orthorhombic $\text{Bi}(\text{Sb}_{0.55}\text{Nb}_{0.225}\text{Ta}_{0.225})\text{O}_4$, which is at the boundary of region I and II, II and III, respectively, were calculated as $a = 5.504(2)\text{ \AA}$, $b = 4.903(3)\text{ \AA}$, $c = 11.892(3)\text{ \AA}$, $\beta = 101.669(1)^\circ$, $V = 314.270(2)\text{ \AA}^3$ and $a = 4.909(4)\text{ \AA}$, $b = 11.765(4)\text{ \AA}$, $c = 5.596(1)\text{ \AA}$, $V = 323.202(3)\text{ \AA}^3$. Fig. 3 shows the schematic crystal structure of monoclinic phase (along ac -plane and bc -plane) and orthorhombic phase (along bc -plane and ab -plane) [5,6]. The phase transformation from the monoclinic to orthorhombic phase can be explained as follows. As x value decreases, the volumes of octahedra increase along with the average ionic radius of B^{5+} , which causes the decrease in the space occupied by Bi^{3+} ions. When x decreases to 0.78, the space occupied by Bi^{3+} ions reaches a minimum. When x decreases further, the atoms’ positions and space structure need to be rearranged to increase or offset the decreasing space occupied by Bi^{3+} ions layer. Then the orthorhombic structure is obtained via the torsion of octahedra and displacement of Bi^{3+} ions layers. The distance between the two neighboring Bi^{3+} ions layers D_m jumps from $11.646(4)\text{ \AA}$ of monoclinic $\text{Bi}(\text{Sb}_{0.78}\text{Nb}_{0.11}\text{Ta}_{0.11})\text{O}_4$ ($D_m = c \times \sin \beta$) to $11.765(3)\text{ \AA}$ of orthorhombic $\text{Bi}(\text{Sb}_{0.55}\text{Nb}_{0.225}\text{Ta}_{0.225})\text{O}_4$ (b value).

Fig. 4 shows the amount of triclinic phase in $\text{Bi}[\text{Sb}_x(\text{Nb}_{0.5-x}\text{Ta}_{0.5-x})\text{O}_4]$ ($0.037 \leq x \leq 0.469$) ceramics as a function of the sintering temperature. First we defined the ratio amount of the triclinic phase as follows. Considering the superposition of the strongest peaks of triclinic ((0 1 2) at 28.27°) and orthorhombic ((1 2 1) at 28.31°) phase, the ratio amount of the triclinic phase was calculated approximately using the following equation:

$$\text{Amount} = \gamma \times I_t / [I_t + I_o] \quad (1)$$

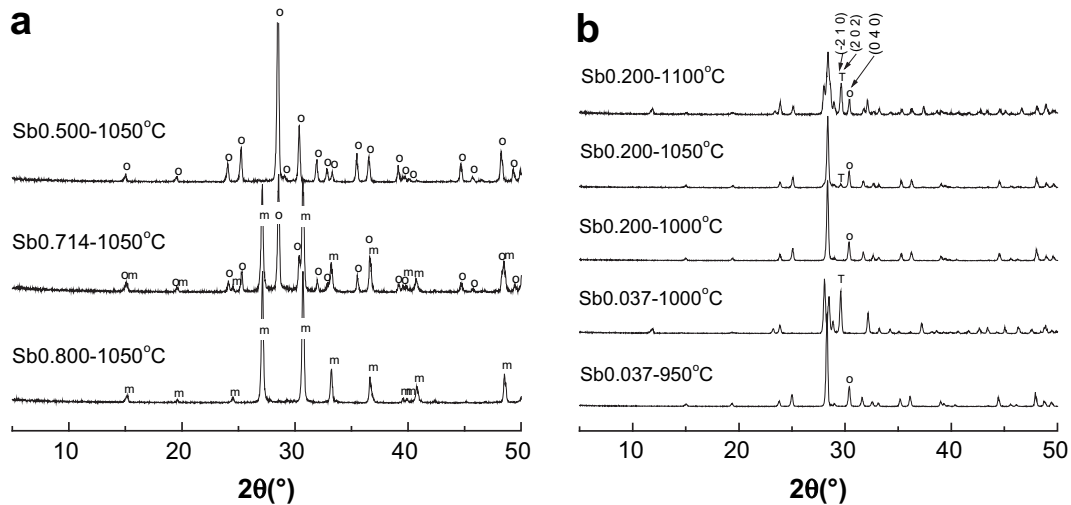


Fig. 2. Typical XRD patterns of monoclinic phase $\text{Bi}(\text{Sb}_{0.8}\text{Nb}_{0.1}\text{Ta}_{0.1})\text{O}_4$, complex phases $\text{Bi}(\text{Sb}_{0.714}\text{Nb}_{0.143}\text{Ta}_{0.143})\text{O}_4$ and orthorhombic phase $\text{Bi}(\text{Sb}_{0.5}\text{Nb}_{0.25}\text{Ta}_{0.25})\text{O}_4$ (a), XRD patterns of $\text{Bi}(\text{Sb}_{0.037}\text{Nb}_{0.4815}\text{Ta}_{0.4815})\text{O}_4$ and $\text{Bi}(\text{Sb}_{0.2}\text{Nb}_{0.4}\text{Ta}_{0.4})\text{O}_4$ compositions sintered at 950–1100 °C demonstrating the phase transformation from orthorhombic to triclinic structure (o – orthorhombic; m – monoclinic; T – triclinic, only characteristic peaks are marked in (b)).

where I_t and I_o are the intensities of the triclinic peaks (2 0 2), (–2 1 0) and orthorhombic peak (0 4 0) respectively as shown in Fig. 2(b) [12–14]. These are the strong and characteristic peaks of the two phases. Considering that the relative strength of triclinic (–2 1 0) is 55 and the relative strength of orthorhombic (0 4 0) is 40, the factor γ is set to 40/55. From the results shown in Fig. 4, we can obtain two basic rules. First, orthorhombic phase started to transform to triclinic phase gradually as the sintering temperature increased and

fully changed to triclinic phase at high temperatures. Single triclinic phase of ABO_4 can be obtained by heating orthorhombic phase to above the phase transformation temperature and triclinic ABO_4 are usually thought to be a more stable structure than the orthorhombic structure because of its smaller cell volume [1–9]. Hence it is not difficult to understand that $\text{Bi}[\text{Sb}_x(\text{Nb}_{0.5}\text{Ta}_{0.5})_{1-x}]\text{O}_4$ ceramics could transform to triclinic phase at high temperature below their melting points. As x value increases, the phase transformation becomes more stable versus sintering temperature as shown in Fig. 4. It means that for a small x value there will be a narrow temperature range for the completion of phase transformation and for a big x value it will take a wider temperature range to complete the phase transformation course, such as that the $\text{Bi}[\text{Sb}_{0.037}(\text{Nb}_{0.5}\text{Ta}_{0.5})_{0.963}]\text{O}_4$ ceramic sharply transformed to triclinic phase between 950 and 1000 °C while the $\text{Bi}[\text{Sb}_{0.2}(\text{Nb}_{0.5}\text{Ta}_{0.5})_{0.8}]\text{O}_4$ ceramic completed its transformation gradually between 1000 and 1150 °C as shown in Fig. 2(b). In fact this tendency was stopped near the melting point. Second, as x value increases it is more difficult for

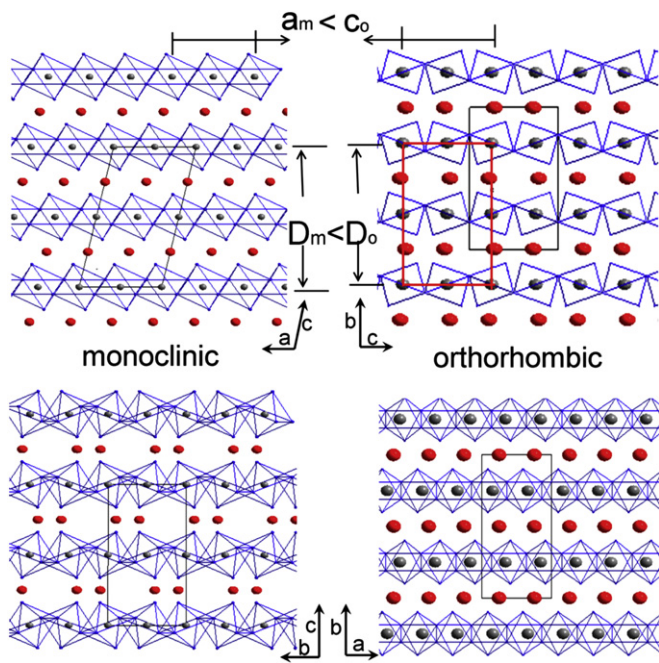


Fig. 3. Schematic illustrations of crystal structure of monoclinic and orthorhombic phase of $\text{Bi}(\text{Sb}_x\text{Nb}_y\text{Ta}_z)\text{O}_4$ ($x + y + z = 1$) (top left corner showing octahedral network of monoclinic structure along the ac -plane, top right corner showing octahedral network of orthorhombic structure along the bc -plane, bottom left corner showing octahedral network of monoclinic structure along the bc -plane, bottom right corner showing octahedral network of orthorhombic structure along the ab -plane, D_m is the distance between two neighboring $\text{B}^{5+}\text{-O}$ octahedra with monoclinic structure and D_o is the distance between two neighboring $\text{B}^{5+}\text{-O}$ octahedra within orthorhombic structure).

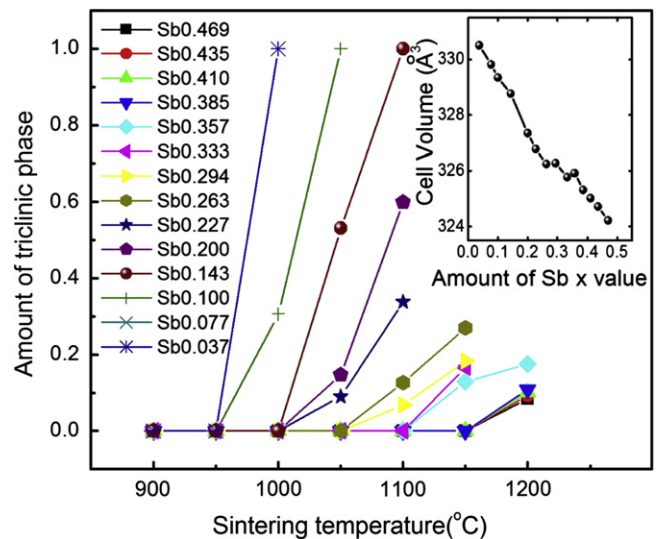


Fig. 4. Amount of triclinic phase in $\text{Bi}[\text{Sb}_x(\text{Nb}_{0.5}\text{Ta}_{0.5})_{1-x}]\text{O}_4$ ($0.037 \leq x \leq 0.469$) ceramics as a function of sintering temperature.

orthorhombic phase to transform to triclinic phase at the same sintering temperature, which means the increase of Sb amount in $\text{Bi}[\text{Sb}_x(\text{Nb}_{0.5}\text{Ta}_{0.5})_{1-x}]\text{O}_4$ restrains the phase transformation from orthorhombic to triclinic. This tendency was especially clear for samples sintered at 1100 °C with x changing from 0.143 to 0.333 as shown in Fig. 4. In other words, phase transformation temperatures increased as the Sb amount increased. Furthermore when $x > 0.2$, even though at melting temperatures the phase transformations were still unfinished. Orthorhombic structure is consisted of two bismuth layers and two separated octahedral layers with different distortions while the triclinic phase is made up of two bismuth layers and two joined octahedron layers. When the sintering temperature is high enough, the two neighboring octahedral layers obtain enough energy to join together and separate the two neighboring bismuth layers beside their sides to reach a more stable structure with a smaller cell volume. The Sb substitution for Nb and Ta reduced the volumes of octahedra and cell volumes. In other words, the Sb substitution stabilizes the orthorhombic structure because of the decrease of cell volume and more energy is needed to complete the phase transformation to triclinic structure.

4. Conclusions

In summary, monoclinic phase region, orthorhombic phase region and their co-existing phase regions are found in a pseudo-ternary phase diagram of the $\text{Bi}(\text{Sb,Nb,Ta})\text{O}_4$ system. The phase transformation from the monoclinic to orthorhombic structure can be attributed to the decrease of space occupied by the bismuth layers, which is caused by the increase of octahedra volumes when the Nb or Ta amount increases. In orthorhombic phase region, as the sintering temperature increases, the phase transformation to triclinic structure is observed and it is seriously affected by the sintering temperature and the Sb amount in $\text{Bi}(\text{Sb,Nb,Ta})\text{O}_4$.

Acknowledgements

This work was supported by the National 973 project of China (2009CB623302), NSFC project of China (60871044, 50835007) and the Key Project of Chinese Ministry of Education (106144).

References

- [1] B. Aurivellius, *Ark. Kemi.* 3 (1951) 153.
- [2] R.S. Roth, J.L. Waring, *J. Res. Natl. Bur. Stand. U.S.* 66A (1962) 451.
- [3] R.S. Roth, J.L. Waring, *Amer. Min.* 48 (1963) 1348.
- [4] E.T. Keve, A.C. Skapski, *Chem. Commun.* (1967) 281.
- [5] E.T. Keve, A.C. Skapski, *J. Solid State Chem.* 8 (1973) 159.
- [6] M.A. Subramanian, J.C. Calabrese, *Mater. Res. Bull.* 28 (1993) 523.
- [7] D. Zhou, H. Wang, X. Yao, X.Y. Wei, F. Xiang, L.X. Pang, *Appl. Phys. Lett.* 90 (2007) 172910.
- [8] P. Ayyub, M.S. Multani, V.R. Palkar, R. Vijayaraghavan, *Phys. Rev. B* 34 (1986) 8137.
- [9] A.W. Sleight, G.A. Jones, *Acta Crystallogr. B* 31 (1975) 2748.
- [10] V.I. Popolitov, A.N. Lobachev, V.F. Peskin, *Ferroelectrics* 40 (1982) 9.
- [11] V.I. Popolitov, R.M. Aliev, *J. Appl. Chem. USSR* 61 (1988) 223.
- [12] H. Kagata, T. Inoue, J. Kato, I. Kameyama, *Jpn. J. Appl. Phys.* 31 (1992) 3152.
- [13] C.L. Huang, M.H. Weng, *Mater. Lett.* 43 (2000) 32.
- [14] N. Wang, M.Y. Zhao, Z.W. Yin, *Mater. Sci. Eng. B* 99 (2003) 238.
- [15] D. Zhou, H. Wang, X. Yao, L.X. Pang, *J. Am. Ceram. Soc.* 91 (2008) 1380.
- [16] D. Zhou, H. Wang, X. Yao, L.X. Pang, *J. Am. Ceram. Soc.* 91 (2008) 2228.
- [17] X.P. Lin, F.Q. Huang, W.D. Wang, K.L. Zhang, *Appl. Catal. A: Gen.* 307 (2006) 257.
- [18] Z.G. Zou, J.H. Ye, H. Arakawa, *Solid State Commun.* 119 (2001) 471.
- [19] Z.G. Zou, J.H. Ye, K. Sayama, H. Arakawa, *Chem. Phys. Lett.* 343 (2001) 303.
- [20] C.F. Yang, *Jpn. J. Appl. Phys.* 38 (1999) 6797.
- [21] C.L. Huang, M.H. Weng, G.M. Shan, *J. Mater. Sci.* 35 (2000) 5443.
- [22] W.C. Tzou, C.F. Yang, Y.C. Chen, P.S. Cheng, *J. Eur. Ceram. Soc.* 20 (2000) 991.
- [23] W. Choi, K.Y. Kim, *J. Mater. Res.* 13 (1998) 2945.
- [24] N. Wang, M.Y. Zhao, Z.W. Yin, *Ceram. Int.* 30 (2004) 1017.
- [25] B. Kennedy, *Powder Diffr.* 9 (1994) 164.
- [26] C.Y. Lee, R. Macquart, Q.D. Zhou, B.J. Kennedy, *J. Solid State Chem.* 174 (2003) 310.
- [27] D. Zhou, H. Wang, X. Yao, L.X. Pang, Y.H. Chen, *Mater. Chem. Phys.* 113 (2009) 265.
- [28] F. Rubio-Marcos, P. Ochoa, J.F. Fernandez, *J. Eur. Ceram. Soc.* 27 (2007) 4125.
- [29] R.D. Shannon, *Acta Crystallogr. A* 32 (1976) 751.